On contribution and detection of higher eigenmodes during dynamic atomic force microscopy

Govind Saraswat and Murti V. Salapaka

Citation: Applied Physics Letters **102**, 173108 (2013); doi: 10.1063/1.4803939
View online: http://dx.doi.org/10.1063/1.4803939
View Table of Contents: http://scitation.aip.org/content/aip/journal/apl/102/17?ver=pdfcov
Published by the AIP Publishing

On contribution and detection of higher eigenmodes during dynamic atomic force microscopy

Govind Saraswat and Murti V. Salapaka[a)]
Department of Electrical and Computer Engineering, University of Minnesota-Twin Cities, Minneapolis, Minnesota 55455, USA

(Received 15 March 2013; accepted 19 April 2013; published online 1 May 2013)

Dynamic mode operation of Atomic Force Microscopes relies on demodulation schemes to get information from different flexure modes of the cantilever while imaging a sample. In the article, we demonstrate that the conventional approach of discerning higher mode participation via amplitude and phase demodulation is not suitable for high bandwidth applications. Furthermore, we provide a method where the higher mode participation is reconstructed with high fidelity, and present a scheme for high bandwidth detection of higher modes when their participation becomes significant. These methods are shown to outperform the traditional amplitude-phase demodulation schemes in terms of speed, resolution, and fidelity. The framework developed is tested on simulations and the method's utility for first two modes is demonstrated experimentally. © *2013 AIP Publishing LLC*.
[http://dx.doi.org/10.1063/1.4803939]

For past few decades, Atomic Force Microscopes[1] (AFMs) have been used for material investigation with unparallel lateral and vertical resolution. One form of the dynamic mode of operation is the *intermittent-contact mode* of AFM, which is among the least invasive modes of probe based investigation. This *intermittent-contact mode* of operation is well-suited for imaging soft-matter which include cells, proteins, and various other biological material. Most of the analysis of the dynamic mode operation is based on the single-mode approximation of the cantilever beam. However, recently, newer modalities of operation are employing higher modes of the cantilever flexure beam[2] and are also using novel means of excitation[3,4] Moreover, a number of soft-matter investigations are conducted in a fluid environment where the quality factors of various modes of cantilever's deflection are significantly lower. The lowered quality factors can enhance[5] the participation of the higher modes in forming the cantilever deflection.

In existing methods for quantifying the contribution of higher modes, the cantilever deflection is demodulated at each mode's resonant frequency and the resulting amplitude and phase are used to quantify the contribution of each mode. These methods extract the frequency content at or near modal frequency of higher modes and ignore the content of the cantilever deflection at frequencies away from the modal frequencies. Also, as amplitude and phase are slowly varying signals (when compared to the modal resonant frequencies), it can be particularly difficult to capture effect of higher modes in the transient and possibly short lived effects of sample on the cantilever deflection. In this letter, we show that the cantilever deflection can have appreciable content at frequencies away from the immediate vicinity of modal resonant frequencies and build a framework to extract such content in real-time. Apart from estimating the participation of higher modes in the cantilever deflection, we provide a high bandwidth method that detects when the higher mode participation is appreciable. Such a detection method is particularly suited for detecting short-lived and transient effects of higher mode participation. Methods built are shown to detect and quantify the contribution of first two modes experimentally.

In *intermittent-contact mode*, it is reasonable to assume that the mode shapes are dictated by the fixed-free boundary conditions. Here, we assume the cantilever to be an unforced Euler-Bernoulli beam with one end fixed (at $x=0$) and another end free (at $x=L$). We also assume that external excitation to the cantilever is provided as a forcing $g(t)$ and the tip sample interaction forcing is given by $\Phi(p,\dot{p})$ at $x=L$ (tip position), where $p(t):=w(L,t)$. Assuming an N mode approximation, with the jth mode shape being $\psi_j(x)$, it can be shown using variational principles[6] that $w(x,t) = \sum_{j=1}^{N} \psi_j(x) q_j(t)$ with each $q_j(t)$ satisfying

$$\frac{\ddot{q}_j}{\omega_j^2} + \frac{\dot{q}_j}{\omega_j Q_j} + q_j = \frac{g_j(t)+\eta_j(t)}{k_j} + \frac{\Phi_j(p,\dot{p})}{k_j}, \tag{1}$$

where $g_j(t) = \psi_j(L) g(t), \Phi_j(p,\dot{p}) = \psi_j(L)\Phi(p,\dot{p}), \eta_j(t)$ is the forcing on the jth mode due to thermal noise; and ω_j, k_j, and Q_j are jth mode's resonant frequency, spring constant, and quality factor, respectively. Each instance of Eq. (1) is a second order ordinary differential equation with external forcing, $f_j := \psi_j(L)(g(t)+\Phi(p,\dot{p}))$, and can be recast as

$$\begin{bmatrix} \dot{x}_{1j} \\ \dot{x}_{2j} \end{bmatrix} = \overbrace{\begin{bmatrix} 0 & 1 \\ -\omega_j^2 & -\dfrac{\omega_j}{Q_j} \end{bmatrix}}^{A_j} \begin{bmatrix} x_{1j} \\ x_{2j} \end{bmatrix} + \overbrace{\begin{bmatrix} 0 \\ \dfrac{\omega_j^2}{k_j} \end{bmatrix}}^{B_j} (f_j + \eta_j),$$
$$y_j = \overbrace{\psi_j(L)\begin{bmatrix} 1 & 0 \end{bmatrix}}^{C_j} \begin{bmatrix} x_{1j} \\ x_{2j} \end{bmatrix}, \tag{2}$$

where state x_{1j} and state x_{2j} denotes the cantilever's jth-mode position and velocity, respectively; and $y_j = \psi_j(L) q_j$ is the contribution of the jth-mode to the cantilever tip deflection p, where $p = \sum_{j=1}^{N} y_j$. Let $B_j^L = B_j \psi_j(L)$, then Eq. (2) can be written as

a)Electronic mail: murtis@umn.edu. URL: nanodynamics.ece.umn.edu

$$\begin{aligned} \dot{x_j} &= A_j x_j + B_j^L(g(t) + \Phi(p,\dot{p})) + B_j \eta_j(t), \\ y_j &= C_j x_j, \end{aligned} \tag{3}$$

where $x_j = [x_{1j} \quad x_{2j}]'$. The model in Eq. (3) can be identified via frequency sweep methods or using thermal noise response near each mode's resonance. This model can be discretized and represented as

$$\begin{aligned} x_j(k+1) &= F_j x_j(k) + G_j^L(g(k) + \Phi(p,\dot{p})) + G_j \eta_j(k), \\ y_j(k) &= H_j x_j(k). \end{aligned} \tag{4}$$

With $x(k) := [x_1(k) \quad x_2(k) \quad \dots \quad x_N(k)]'$, Eq. (4) for each value of $j = 1, 2, \dots, N$ can be combined and written as

$$\begin{aligned} x(k+1) = &\underbrace{\begin{bmatrix} F_1 & \cdots & 0 \\ 0 & \ddots & 0 \\ 0 & 0 & F_N \end{bmatrix}}_{F} x(k) + \underbrace{\begin{bmatrix} G_1^L \\ \vdots \\ G_N^L \end{bmatrix}}_{G^L} (g(k) + \Phi(p,\dot{p})) \\ &+ \underbrace{\begin{bmatrix} G_1 & \cdots & 0 \\ 0 & \ddots & 0 \\ 0 & 0 & G_N \end{bmatrix}}_{G} \underbrace{\begin{bmatrix} \eta_1(k) \\ \vdots \\ \eta_N(k) \end{bmatrix}}_{\eta(k)}, \\ y(k) = &\underbrace{[H_1 \quad \cdots \quad H_N]}_{H} x(k) + \nu(k). \end{aligned} \tag{5}$$

Here, all η_j's are independent and Gaussian. Let the covariance matrix of the thermal noise vector η be given by $E(\eta\eta^*) = S$. Also ν characterizes the measurement (photodiode) noise with covariance $E(\nu\nu^*) = R$.

The multi-mode model of the cantilever described above in Eq. (5) was used to study the first two flexure modes of an Olympus AC240 (Product Id# OMCL-AC240TS) cantilever. The multi-mode cantilever dynamics was identified experimentally using the frequency sweep method where the first mode resonant frequency was determined to be at 75.8 kHz and second mode resonant frequency at 457.6 kHz. The cantilever and its interaction with sample was simulated, where a piece-wise linear model[7] of the tip-sample interaction was assumed. Here, the cantilever was excited at its first resonance frequency, with a free-air (when there is no sample) amplitude of 200 nm. Each mode's contribution (y_j) to the cantilever deflection was analyzed. Figure 1 compares the power spectrum of the second mode signal y_2 when the cantilever is interacting with the sample of height 30 nm to when it is oscillating freely (free-air). It is evident from Figure 1 that in the absence of the sample, only the modal frequencies have appreciable impact on the cantilever deflection. Here, the first peak in the spectrum of the deflection measurement is caused primarily by the forcing, whereas the second peak is a result of the thermal noise. In the presence of the sample, the nonlinear interaction spreads the energy being injected at the first resonant frequency into many harmonics of the forcing. Moreover, the sixth harmonic resonates with the second modal frequency of the cantilever resulting in an appreciable peak near the second modal frequency. We remark that apart from the sixth harmonic of the forcing frequency, other harmonics also get a boost due to the way the entire frequency response of the two-mode model of the cantilever amplifies

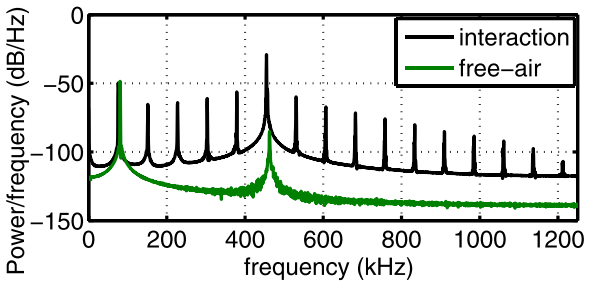

FIG. 1. Simulation results showing cantilever 2nd-mode power spectrum before and after interaction with a sample of height 30 nm. Free-air curve is shifted right by 5 kHz to highlight the difference in peaks.

the harmonics. In a typical scheme based on demodulation near modal frequencies, these other harmonics get ignored where possibly important information is lost. Furthermore, here the role played by the second and the first modes cannot be clearly delineated.

Indeed, it is worth mentioning here that for a higher mode extension of the multi-frequency excitation (like such used by Agarwal and Salapaka[3]), it is essential to obtain the entire trajectory of each mode. As alluded to earlier, all modes contribute to the total gain for each harmonics and thus a simple demodulation scheme at each of the harmonic cannot be used to separate the cantilever deflection signal into each mode's contribution. Amplitude-phase demodulation schemes thus fall short for such operations. Next we present an observer based framework to address these challenges.

In a typical multimode operation of the dynamic mode, lock-in amplifiers are used to extract the amplitude of each mode from the measured tip deflection. We propose observer based state-detection scheme that has the capability of incorporating effects away from the modal frequency. We subsequently develop a fast detection method of higher mode participation in the measured deflection signal. The proposed scheme relies on the construction of a dynamic Kalman observer for linear system of Eq. (5) that provides an estimate, $\hat{x}(k+1)$ of the state x of the cantilever, depending on all the observations till time step k, and is given by

$$\begin{aligned} \hat{x}(k+1) &= F\hat{x}(k) + \overbrace{FP_kH'(HP_kH' + R)^{-1}}^{L_k} \\ &\quad [y(k) - \hat{y}(k)] + G^L g(k), \\ \hat{y}(k) &= H\hat{x}(k), \\ P_{k+1} &= F[I - P_kH'(HP_kH' + R)^{-1}H] \\ &\quad P_kF' + GSG', \end{aligned} \tag{6}$$

with $\hat{x}(0) = 0$ and the *error covariance* $P_k := Cov(x(k) - \hat{x}(k))$ initialized by a large number P_0, depending on actual state values. The observer (Eq. (6)) mimics the dynamics of the cantilever (Eq. (5)) and utilizes a correcting term $L_k e$, where L_k is the observer gain and $e := H\tilde{x} := H(x - \hat{x})$ is called the error innovation (difference between estimated and actual output). The error dynamics in absence of tip-sample interaction is given by

$$\tilde{x}(k+1) = (F - L_kH)\tilde{x}(k) + G\eta(k) - L_k\nu(k). \tag{7}$$

Due to low measurement noise, it is possible to choose L_k,[8] such that the real part of the eigenvalues of $(F - L_k H)$ can have large negative value and thus $\tilde{x}$ goes to zero fast in absence of noise. Also the estimate of the contribution of the jth mode, $\hat{y}_j$ can be obtained via

$$\hat{y}_j(k) = \underbrace{[0 \ \cdots \ H_j \ \cdots \ 0]}_{\text{only } j\text{-th element non-zero}} \hat{x}(k). \tag{8}$$

With further analysis of the observer, it was found that the error covariance P_k reaches a constant value fast (depending on the noise covariances). Here, the dynamic kalman observer behaves as a steady-state observer where the cantilever behavior in the past over a long time horizon has undue influence on the estimation of the current state of the cantilever. During dynamic AFM operation, when tip-sample interaction length changes suddenly there is a significant error in estimation if the steady-state Kalman gain is used. This suggests that filter gains should be suitably altered for fast tracking. To address the above issue, we employ a receding horizon Kalman[9] (RHK) observer which provides an estimate $\hat{x}_{rh}(k)$ of the state $x(k)$ based on the past M photodiode measurements and ignoring the rest of the measurement history. The value of M is suitably chosen to balance the effect of noise and the responsiveness of the estimation to fast changes in the state. Dynamics of the RHK observer is given by Eq. (6), but for each time-instant k, $\hat{x}_{rh}(k)$ is estimated by following the dynamics of Eq. (6) initialized at $(k-M)^{th}$ instance as $\hat{x}_{rh}(k-M) = 0$ and $P_{k-M} = P_0$. The designed RHK observer results in observer gains that adapt to sudden tip-sample interactions and is thus able to track changes in the state of the cantilever faster than the steady-state observer.

To demonstrate the utility of the observer, simulations were performed using the setup given earlier. Cantilever model was excited at its first resonance frequency, with a free-air amplitude of 200 nm and a step of 30 nm was given to the sample height. Trajectories of the second mode were reconstructed using both amplitude-phase demodulation of the cantilever deflection (using lock-in amplifier) and via two types of observers; steady-state and the RHK observer. M was chosen to be 10 for this simulation. The RHK observer performed better than the steady-state observer and thus only results obtained using the RHK observer are presented here. Figure 2(a) plots the root-mean-square (rms) error between actual trajectory y_2 of the cantilever and with those reconstructed via RHK observer (RHK) and via amplitude-phase demodulation (Lock-In). It is evident that after each tip-sample interaction (one cycle of excitation frequency), error in trajectory estimated via observer reduces to zero fast (within a couple of cycles of second mode resonant frequency), whereas the trajectory constructed using Lock-in is not able to capture the transients and results in an increasing error till transients die out. We remark that often,[5] the effect on the second mode can be limited to the transient part of the response and thus it is possible in such cases that the entire signature of the sample's influence on the second mode cannot be accurately tracked using demodulation based schemes. It is also evident that the demodulation scheme is not able to capture the actual 2nd−mode trajectory

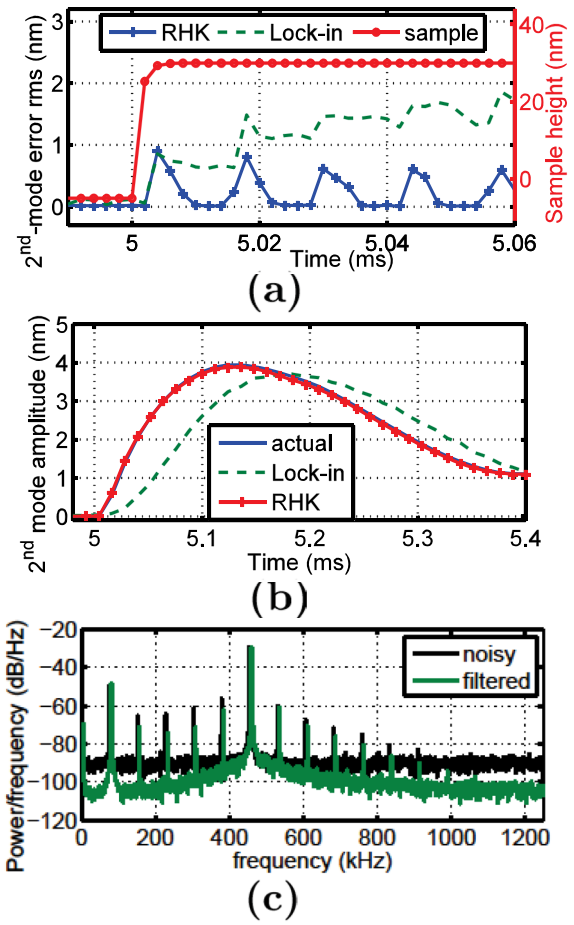

FIG. 2. Simulation results showing cantilever 2nd-mode response for a step change in sample height. (a) rms of error between actual and estimated 2nd-mode trajectories, by both amplitude-phase demodulation using lock-in amp (green) and RHK observer (blue). Sample height is changed from no-interaction (shown with negative value) to an interaction of 30 nm at the time instant of 5 s. The RHK observer is able to track the 2nd-mode trajectory in less than 0.01 ms after every tip-sample interaction, and thus, has a tracking bandwidth of more than 100 kHz. (b) 2nd-mode amplitude demodulated from y_2 (without any measurement noise, blue), RHK observer estimate $\hat{y}_2$ (red) and y (combined cantilever deflection, green). Amplitude demodulated from RHK observer overlaps with the actual contribution. Rise time of actual amplitude is ≈0.12 ms, whereas the rise time of lock-in amplitude is ≈0.18 ms. (c) Power spectrum for the noisy measurement of the 2nd-mode contribution and its estimate.

with high fidelity as there is no tracking for the time the appreciable second mode contribution is present. Figure 2(c) shows the power spectrum of $(y_2 + \nu)$ and the estimate $\hat{y}_2$. The observer is able to filter the noise with more than 20 dB per decade attenuation before 600 kHz, while keeping the peaks at the 1st and 2nd modal frequencies intact. Peaks at the harmonics of the excitation frequency are also present but slightly attenuated. These peaks are ignored and lost when using demodulation. As the noise in the estimated $\hat{y}_2$ is significantly reduced, demodulation of $\hat{y}_2$ at the second modal frequency can have much higher bandwidth which is not possible for direct demodulation of the measured noisy cantilever deflection. Figure 2(b) shows the 2nd-mode demodulated amplitudes where the one estimated from RHK observer (termed as RHK amplitude) is overlapping the actual 2nd-mode amplitude. It is clear from these simulations that the RHK observer is able to track the 2nd-mode contribution within 2–3 cycles of second mode resonant frequency,

which can be translated into a tracking bandwidth of more than 100 kHz. This is an *order of magnitude improvement* compared to amplitude-phase demodulation based methods (typical bandwidth of no more than 10 kHz).

The advantages of observer based reconstruction of second mode trajectories are further demonstrated by experiments using an Olympus AC240 cantilever for the dynamic mode imaging on Mica. Here, the setpoint amplitude was 203 nm with free-air amplitude being 240 nm. Parameters of the cantilever, characterized for the first two modes are

- $k_1 = 1.72\,\text{N/m}$, $\omega_1 = 151.6\pi$ rad/s, $Q_1 = 168$, $\omega_2 = 915.2\pi$ rad/s and $Q_2 = 478$.

Freshly cleaved Mica sample was attached to a small piezoscanner and square pulses of various amplitude and frequencies were applied to the piezoscanner. Each pulse applied to the piezo moved the mica sample up and down and generated a square sample profile of height 10 nm. A feedback loop on z-axis with very low controller gains was used to cancel any drift. Deflection and dither forcing signals were captured and sampled at 2.5 MHz and were analyzed offline. Trajectory of 2nd- mode was estimated using the RHK observer and the demodulated amplitude is plotted in Figure 3 along with the direct demodulation of the measured deflection signal. Here, the actual 2nd-mode trajectory is not known and thus rms error plot of Figure 2(a) cannot be plotted. However, similar to the simulation result from Figure 2(b), the amplitude demodulated from the estimated $\hat{y}_2$ has a faster response, with a rise time approximately half of the Lock-in based amplitude.

Here, we have provided a method that reconstructs the relative modal participation of an AFM cantilever using observers and have demonstrated that significant gains can be accrued in the fidelity and bandwidth of higher model participation. Further gains can result if the purpose is to simply *detect* if higher mode participation is significant or not without emphasizing its magnitude. To enable faster detection of higher modes, we model the tip-sample interaction as a force that possibly appears every cycle of the cantilever oscillation. The interaction is short-lived, and is appreciable only when the cantilever is near the sample-surface. Assuming an impulsive force as a model for the short-lived force (which is valid when compared to the entire trajectory of the cantilevers orbit), we can model the dynamics as given by[10,11]

$$x(k+1) = Fx(k) + G^L g(k) + G\eta(k) + \delta_{\theta,k+1} v, \tag{9}$$

where $\delta_{l,k}$ denotes the dirac delta function, θ is the time-instance of the impact (a hit), and $v = [v_1 \ldots v_N]'$ is the magnitude of impact, measured in the amount of change in the state of each respective mode. In this case, error e for steady state observer with gain $L = [L_1 \ldots L_N]'$ is given by

$$e(k) = \sum_{j=1}^{N} \Gamma_j(\theta, k) v_j + e_0(k), \tag{10}$$

where

$$\Gamma_j(\theta, k) = [H_j(F_j - L_j H_j) \ldots H_j(F_j - L_j H_j)^{k-\theta}]'. \tag{11}$$

Assuming each dynamic profile Γ_j can be approximated by M_1 samples with $\bar{\Gamma}_j = \Gamma_j(k - M_1, k)$, $\bar{e}(k) = [e(k); \ldots; e(k - M_1 - 1)]$, and $\bar{e}_0(k) = [e_0(k); \ldots; e_0(k - M_1 - 1)]$, Eq. (10) can be written as

$$\bar{e}(k) = \underbrace{[\bar{\Gamma}_1 \ldots \bar{\Gamma}_N]}_{\Gamma_{eq}} \begin{bmatrix} v_1 \\ \vdots \\ v_N \end{bmatrix} + \bar{e}_0(k). \tag{12}$$

For Kalman observer, as $\bar{e}_0(k)$ is *white noise*,[12] the impact of tip-sample interaction v can be estimated by a *linear unbiased estimator*[13] given by

$$\begin{bmatrix} v_1 \\ \vdots \\ v_N \end{bmatrix} = (\Gamma'_{eq}\Gamma_{eq})^{-1}\Gamma'_{eq}\bar{e}(k). \tag{13}$$

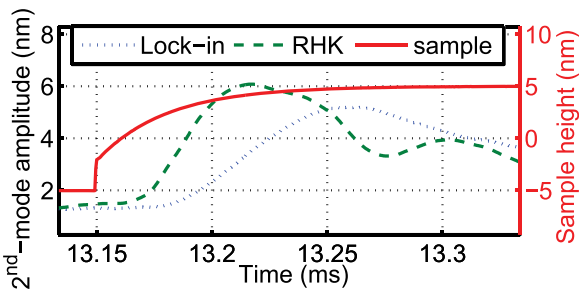

FIG. 3. Experimental result for a 10 nm step change in sample height. 2nd mode amplitudes demodulated from trajectory estimated via Kalman observer (RHK) compared with that evaluated by demodulation of the cantilever deflection (Lock-in). Rise time of RHK amplitude is ≈0.05 ms, whereas the rise time of lock-in amplitude is ≈0.1 ms which is of similar order to as observed in simulation.

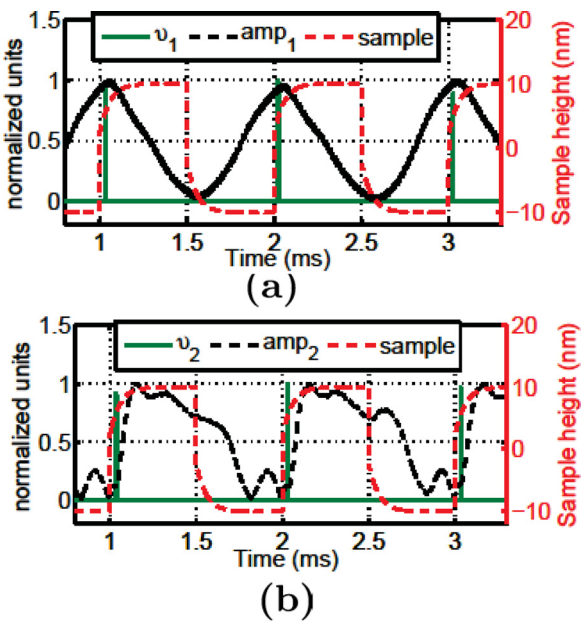

FIG. 4. Experimental result for higher mode detection. A square pulse of 20 nm and 1 kHz frequency was given to the sample height. (a) shows sample height overlaid on the 1st mode amplitude (blue) and the detected "hits." Green curve peaks are the local maxima of v_1 identifying the time of impact and also quantifying the effect of impact on the 1st-mode. (b) shows the local maxima of v_2 with second mode amplitude overlaid.

Experiments were performed on the experimental setup described earlier where a sample with a square profile of 20 nm was imaged. The Kalman observer was used to obtain the *innovation* signal and the v_1 and v_2 were found using Eq. (13). Figures 4(a) and 4(b) plot the time of impact for 1st two modes and there normalized value along with the respective amplitudes and the sample height. Both modes are detected within two to three cycles of exciting frequency. As excitation is near the first mode, the detection bandwidth of detector is from half to third of the first modal frequency translating into a detection bandwidth of ≈20 kHz. The natural bandwidth of j-th mode of the cantilever is bounded by $\beta_j := (\omega_j/Q_j)$ which is considerably small for first few modes ($\beta_1 \approx 350$ Hz and $\beta_2 \approx 955$ Hz for the used cantilever). Thus, the detection method developed here is able to improve speed of detection of first two modes by ≈20 times.

The work was supported by NSF under the Award No. ECCS 1202411 to M.S.

[1]G. Binnig, C. F. Quate, and C. Gerber, Phys. Rev. Lett. **56**, 930 (1986).
[2]N. Martinez, S. Patil, J. Lozano, and R. Garcia, Appl. Phys. Lett. **89**, 153115 (2006).
[3]P. Agarwal and M. Salapaka, Appl. Phys. Lett. **95**, 083113 (2009).
[4]R. Garcia and E. T. Herruzo, Nat. Nanotechnol. **7**, 217 (2012).
[5]X. Xu, J. Melcher, S. Basak, R. Reifenberger, and A. Raman, Phys. Rev. Lett. **102**, 060801 (2009).
[6]M. V. Salapaka, H. S. Bergh, J. Lai, A. Majumdar, and E. McFarland, J. Appl. Phys. **81**(6), 2480 (1997).
[7]A. Sebastian, M. V. Salapaka, D. Chen, and J. P. Cleveland, J. Appl. Phys. **89**(11), 6473 (2001).
[8]B. Anderson and J. Moore, *Optimal Filtering* (Prentice-Hall, Englewood Cliffs, NJ, 1979).
[9]W. Kwon, P. Kim, and P. Park, IEEE Trans. Autom. Control **44**, 2115 (1999).
[10]D. R. Sahoo, A. Sebastian, and M. V. Salapaka, Appl. Phys. Lett. **83**, 5521 (2003).
[11]D. Sahoo and M. V. Salapaka, in *44th IEEE Conference on Decision and Control* (2005), pp. 1185–1190.
[12]A. S. Willsky and H. L. Jones, IEEE Trans. Autom. Control **21**, 108–112 (1976).
[13]T. Kailath, A. H. Sayed, and B. Hassibi, *Linear Estimation* (Prentice Hall, New Jersey, 2000).